ACTIVATION OF TRANSIENT RECEPTOR POTENTIAL VANILLOID-3 INHIBITS HUMAN HAIR GROWTH

Journal:	*Journal of Investigative Dermatology*
Manuscript ID:	JID-2010-0818.R2
Manuscript Type:	Original Article
Date Submitted by the Author:	18-Feb-2011
Complete List of Authors:	Borbiro, Istvan; University of Debrecen, Medical and Health Science Center, Department of Physiology Lisztes, Erika; University of Debrecen, Medical and Health Science Center, Department of Physiology; Abiol Ltd, none Toth, Balazs; University of Debrecen, Medical and Health Science Center, Department of Physiology Czifra, Gabriella; University of Debrecen, Medical and Health Science Center, Department of Physiology Olah, Attila; University of Debrecen, Medical and Health Science Center, Department of Physiology Szollosi, Attila; University of Debrecen, Medical and Health Science Center, Department of Physiology Szentandrassy, Norbert; University of Debrecen, Medical and Health Science Center, Department of Physiology Nanasi, Peter; University of Debrecen, Medical and Health Science Center, Department of Physiology Peter, Zoltan; University of Debrecen, Medical and Health Science Center, Department of Dermatology Paus, Ralf; University of Lï¿½beck, Department of Dermatology Kovacs, Laszlo; University of Debrecen, Medical and Health Science Center, Department of Physiology Biro, Tamas; University of Debrecen, Medical and Health Science Center, Department of Physiology; Abiol Ltd, none
Key Words:	human organ-cultured scalp hair follicle, hair growth, proliferation, apoptosis, catagen

ACTIVATION OF TRANSIENT RECEPTOR POTENTIAL VANILLOID-3 INHIBITS HUMAN HAIR GROWTH

István Borbíró[1,2], Erika Lisztes[1,2], Balázs I. Tóth[1], Gabriella Czifra[1], Attila Oláh[1], Attila G. Szöllősi[1], Norbert Szentandrássy[1], Péter P. Nánási[1], Zoltán Péter[3], Ralf Paus[4], László Kovács[1], and Tamás Bíró[1,2]

[1]Department of Physiology and [3]Dermatology, University of Debrecen, Medical and Health Science Center, Research Center for Molecular Medicine, Debrecen, Hungary

[2]Abiol Ltd, Debrecen, Hungary

[4]Department of Dermatology, University Hospital Schleswig-Holstein, University of Lübeck, Lübeck, Germany

Corresponding author

Tamás Bíró, M.D., Ph.D.

Department of Physiology, University of Debrecen, Medical and Health Science Center, Research Center for Molecular Medicine, 4032 Debrecen, Nagyerdei krt. 98. PO Box 22, Hungary, Email: biro@phys.dote.hu, Phone: +36-52-255-575, FAX: +36-52-255-116

Short title: TRPV3 inhibits human hair growth

Non-standard abbreviations: 2-APB: 2-aminoethoxydiphenyl borate, HFs: hair follicles, ORS: outer root sheath, TRPV3: transient receptor potential vanilloid-3

ABSTRACT

In the current study, we aimed at identifying the functional role of transient receptor potential vanilloid-3 (TRPV3) ion channel in the regulation of human hair growth. Using human organ-cultured hair follicles (HF) and cultures of human outer root sheath (ORS) keratinocytes, we provide the first evidence that activation of TRPV3 inhibits human hair growth. TRPV3 immunoreactivity was confined to epithelial compartments of the human HF, mainly to the ORS. In organ culture, TRPV3 activation by plant-derived (e.g. eugenol, 10-1000 μM) or synthetic (e.g. 2-aminoethoxydiphenyl borate, 1-300 μM) agonists resulted in a dose-dependent inhibition of hair shaft elongation, suppression of proliferation, and induction of apoptosis and premature HF regression (catagen). Human ORS keratinocytes also expressed functional TRPV3, whose stimulation induced membrane currents, elevated intracellular calcium concentration, inhibited proliferation, and induced apoptosis. Of great importance, these effects on ORS keratinocytes were all mediated by TRPV3 since siRNA-mediated silencing of TRPV3 effectively abrogated the cellular actions of the above agonists. These findings collectively support the concept that TRPV3 signaling is a significant novel player in human hair growth control. Therefore, TRPV3 and the related intracellular signaling mechanism might function as a promising, novel target for pharmacological manipulations of clinically relevant hair growth disorders.

INTRODUCTION

Members of the large transient receptor potential (TRP) ion channel family function as “polymodal cellular temperature sensor” molecules. Indeed, these channels were shown to be involved in sensation of e.g. temperature challenges, chemical irritants, osmolarity, taste, pain, itch, etc. (Clapham, 2003; Nilius et al., 2007; Szállási and Blumberg, 1999; Caterina and Julius, 2001; Paus et al., 2006a; Bíró et al., 2007).

Emerging results of the past decade, however, have suggested that roles of TRP channels are, by no means, restricted to sensory neuron-coupled processes. Stimulated not the least by our pioneering studies with TRPV1 (the “capsaicin receptor” of the vanilloid subgroup) on glial and mast cells (Bíró et al., 1998a, 1998b), it has now become clear that functional TRP channels are also expressed on many different non-neuronal cell types. In the skin, TRPV1 was identified on human epidermal and hair follicle keratinocytes, sebocytes, mast cells, and dendritic cells (Denda et al., 2001; Southall et al., 2003; Bodó et al., 2004). We have also shown that TRPV1 activation suppressed *in vitro* human hair growth, inhibited proliferation of epidermal keratinocytes and sebocytes, induced apoptosis of skin cells, and inhibited lipid synthesis of sebocytes (Bodó et al., 2005; Tóth et al., 2009b). Finally, we have detected a significant delay in hair follicle cycling of TRPV1 KO mice compared to the wild-type control (Bíró et al., 2006). These findings have introduced TRPV1 as a significant novel player in human (and murine) skin and hair growth control, and suggested that TRP channels and their endogenous ligands may represent additional players in the neuroendocrine network of the skin (Slominski and Wortsman, 2000).

Intriguingly, another thermosensitive TRP channel, i.e. TRPV3, which is abundantly expressed in murine keratinocytes (Xu et al., 2002; Smith et al., 2002; Peier et al., 2002; Moussaieff et al., 2008), was recently also implicated in the regulation of murine epidermal and hair growth. It was also shown that a constitutively active, "gain-of-function" mutation of the *trpv3* gene resulted in a hairless phenotype in mice (and rats) (Asakawa et al., 2006; Xiao et al., 2008). Finally, an elegant study (Cheng et al., 2010) has recently demonstrated that TRPV3-coupled signaling mechanisms are key regulators of epidermal growth factor-induced murine hair morphogenesis and skin barrier formation.

Although these interesting data strongly suggested that TRPV3 (similar to TRPV1) may play a profound regulatory role in *murine* hair growth (Steinhoff and Bíró, 2009); moreover, although expression of TRPV3 was identified in the human skin *in situ* (Xu et al., 2002; Gopinath et al., 2005; Facer et al., 2007), we lack data on its function in *human* hair growth control. Therefore, in the current study, we aim at defining whether TRPV3-coupled signaling is involved in the regulation of human hair growth and cycling. Specifically, we intended to identify the expression of TRPV3 in human organ-cultured hair follicles (HF) and in primary cultures of HF-derived outer root sheath (ORS) keratinocytes using immunolabeling and quantitative "real-time" PCR. Furthermore, using a wide-array of functional assays and molecular imaging, we have evaluated the effects of plant-derived and synthetic TRPV3 activators on hair shaft elongation, intrafollicular and ORS keratinocyte proliferation and apoptosis, HF cycling, intracellular ionic homeostasis, and channel activity. Finally, we have analyzed the TRPV3-specificity of the observed cellular actions of the TRPV3 agonists using RNA-interference.

Collectively, our study provides the first evidence that activation of TRPV3 inhibits human hair growth which findings strongly argue for that TRPV3 and the related intracellular signaling mechanism might function as a promising, novel target for pharmacological manipulations of clinically relevant hair growth disorders.

RESULTS

Human scalp HF express TRPV3 mainly in the ORS

First, we intended to define TRPV3 expression in the human HF *in vivo*, using full-thickness normal scalp skin obtained during routine plastic surgery. As revealed by immunohistochemistry, TRPV3-immunoreactivity (ir) in human scalp HF in anagen VI stage of the hair cycle (Paus and Cotsarelis, 1999; Stenn and Paus, 2001) was restricted mostly to the keratinocyte layers of the ORS and, to lesser extent, to the matrix of the HF (**Figure 1a**). In good accord with these data, a strong TRPV3-ir was observed on cultured ORS keratinocytes, both by immunocytochemistry (**Figure 1b**) and Western blotting (**Figure 1c**). The specificity of the immunosignal was assessed by numerous positive and negative controls (see also *Materials and methods* section for details).

In order to control whether intraepithelial TRPV3-ir corresponded to the presence of TRPV3 transcripts, RNA was rapidly extracted from freshly microdissected proximal human anagen HFs and from ORS keratinocyte cultures and then samples were subjected to Q-PCR. As shown in **Figure 1d**, mRNA transcripts for TRPV3 were unambiguously identified both in normal human scalp HF and in HF-derived ORS keratinocytes suggesting that the human HF epithelium indeed transcribes the TRPV3 gene *in vivo*.

In these experiments, two other important findings have been revealed. First, TRPV3-ir (**Figure 1a**) and specific mRNA transcripts (**Figure 1d**) were absent from the

inductive, specialized HF mesenchyme, the fibroblasts of the dermal papilla (DP) as well as from human dermal fibroblast (HDF) (**Figure 1d**) used as feeder layers for the ORS keratinocyte cultures. Second, expression of TRPV3 in the ORS and matrix keratinocyte layers of the human HF appeared to be not regulated by the cycling machinery of the HF since the levels of TRPV3-specific mRNA transcripts (**Figure 1d**) and ir (data not show) were essentially the same in anagen and in spontaneously transformed catagen HFs.

TRPV3 stimulation inhibits hair shaft elongation and hair matrix keratinocyte proliferation, and induces apoptosis-driven premature catagen regression

In order to explore the functional consequences of TRPV3 stimulation *in vitro* under as physiological conditions as possible, microdissected, organ-cultured normal anagen VI scalp HF were exposed to various TRPV3 agonists (Xu et al., 2006; Chung et al., 2004a). Plant-derived agents such as eugenol (**Figure 2**), thymol, and carvacrol (data not shown) – major components of clove, thyme, and oregano – and well as the synthetic agonist 2-APB significantly inhibited hair shaft elongation in a time- and dose-dependent manner (**Figure 2a**).

Hair growth inhibition was further confirmed by the finding that treatment of cultured HFs by these activators for 5 days significantly decreased the number of Ki67+ keratinocytes in the anagen hair bulb (**Figure 2b**). Of further importance, the above agents significantly increased the number of TUNEL+ keratinocytes in the hair bulb after stimulation, suggesting the induction of apoptosis by TRPV3 stimulation (**Figure 2b**).

Using quantitative histomorphometry of HE-staining section of HF and analyzing such staining based on well-defined morphological criteria (Stenn and Paus, 2001; Müller-Röver et al., 2001), we next assessed the effect of the TRPV3 agonists on HF cycling *in vitro*, namely on the anagen-catagen transition, which is characterized by massive up-regulation of keratinocyte apoptosis and down-regulation of keratinocyte proliferation in the anagen hair bulb (Stenn and Paus, 2001; Müller-Röver et al., 2001; Lindner et al., 1997). As shown in **Figure 2c**, the agonists stimulated the onset of catagen transformation of the HF; whereas in the control, most of the HF (>80 %) were in the anagen VI phase, after 8 days of treatment with eugenol or 2-APB, 60-100% of the HF had entered catagen (**Figure 2c**). It should be noted, however, that these TRPV3 agonists were largely capable of inducing only early catagen stages, and that we very rarely found that HF regression *in vitro* had progressed into late stages of the catagen transformation after application of these agents.

TRPV3 is expressed as a Ca^{2+}-permeable ion channel on ORS keratinocytes

Although the above data argued for the functional expression of TRPV3 in keratinocyte layers of the human HF, to further analyze the functionality of the TRPV3 channel, a series dynamic imaging and electrophysiology experiments were performed on primary cultures of human ORS keratinocytes which, as we have shown above (**Figure 1**), express TRPV3-specific mRNA transcripts and proteins.

As revealed by FLIPR-based Ca^{2+}-imaging (Tóth et al., 2009b; Marincsák et al., 2008), TRPV3 agonists markedly increased $[Ca^{2+}]_{ic}$ in a dose-dependent manner

(**Figure 3a and b**). Of further importance, suppression of [Ca^{2+}] of the culturing medium (from 1.8 mM to 0.02 mM) or co-application of 10 μM ruthenium red (a non-selective channel blocker) (Amann and Maggi, 1991) almost fully prevented the actions of the TRPV3 agonists to elevate $[Ca^{2+}]_{ic}$ (**Figure 3b**) suggesting that these agents opened a Ca^{2+}-permeable conductance at the surface membrane of the ORS keratinocytes.

To further assess this phenomenon, patch-clamp (whole cell configuration) experiments were performed. Since membrane currents elicited by square pulses activated quickly and showed no time and voltage dependent inactivation (data not shown), currents were initiated by ramp protocols (**Figure 3c**), applied in every 3 sec. Control (i.e. vehicle-treated) ORS keratinocytes showed outwardly rectifying currents with an average reversal potential of –12.6±1.5 mV (mean±SEM, n=7). Currents were measured and normalized to cell membrane capacitance at four different potential during the ramp protocol, i.e. at –90, –40, +40 and +90 mV resulting –9.5±2.5, –3.5±1.0, 6.2±1.0, and 15.9±3.5 pA/pF, respectively (all data are mean±SEM values) (**Figure 3e**).

Of great importance, both inward and outward currents were markedly and significantly ($p<0.05$) increased by 100 μM 2-APB (**Figure 3c-f**) which effect was reversible. In the presence of 2-APB, the currents measured at –90, –40, +40 and +90 mV were –31.9±14.2, –13.8±6.4, 17.3±6.1, and 57.7±16.6 pA/pF, respectively (mean±SEM, n=7). In average, the TRPV3 activator approximately tripled both inward and outward currents at all potentials. (Notably, all other plant-derived TRPV3 activator exerted similar effects; data not shown). We have also shown that 10 μM

ruthenium red markedly (by 62%, measured at +90 mV, n=3) suppressed the amplitude of the 2-APB-induced current (data not shown).

Collectively, these data unambiguously argue for that human HF-derived ORS keratinocytes indeed express functional TRPV3 which operates as a Ca^{2+}-permeable (most probably non-selective cation) channel at the plasma membrane of the cells, similar to as had previously been described on various epidermal keratinocyte populations (Peier et al., 2002; Cheng et al., 2010; Chung et al., 2004a, 2004b; Huang et al., 2008).

TRPV3 stimulation suppresses proliferation of ORS keratinocytes and induces cell death

Since TRPV3 stimulation of organ-cultured HFs inhibited hair shaft elongation and intrafollicular proliferation and induced apoptosis (**Figure 2**), we next investigated the cellular effects of TRPV3 activation on growth and survival of human ORS keratinocytes. In good accord with these data, as revealed by a wide-array of FLIPR-based functional assays, eugenol and 2-APB suppressed cellular growth of ORS keratinocytes in a dose-dependent manner (**Figure 4a-c**). In addition, the TRPV3 activators markedly suppressed the mitochondrial membrane potential (**Figure 4a-c**), one of the earliest hallmarks of apoptosis (Green and Reed, 1998; Susin et al., 1998). Finally, highest concentrations of the agents were also able to significantly ($p<0.05$) increase Sytox Green accumulation (**Figure 4a**), a sensitive indicator of necrosis/cytotoxicity (Tóth et al., 2009b; Dobrosi et al., 2008).

Of further importance, the growth-inhibitory and cell death-inducing actions of the TRPV3 activators were markedly abrogated by suppression of [Ca^{2+}] of the culturing medium (from 1.8 mM to 0.02 mM) or co-application of 10 μM ruthenium red (**Figure 4b and c**), further arguing for that these cellular actions are mediated by the opening of the surface membrane TRPV3 ion channels and the resulted Ca^{2+}-influx to the ORS keratinocytes.

However, several lines of evidence suggest that the above agents may also activate other TRP channels (Bíró et al., 2007; Xu et al., 2006). Furthermore, we lack highly selective and commercially available TRPV3 inhibitors. Therefore, in order to further assess and verify the TRPV3-specificity of the above cellular responses, a series of TRPV3-targeted RNAi knock-down experiments were carried out in accordance with the techniques developed in our previous studies and which were optimized for various cultured human skin cells (Tóth et al., 2009b; Dobrosi et al., 2008; Griger et al., 2008). (The evaluation of efficacy of the RNAi knock-down is shown in **Supplementary Figure 1.**) Of greatest importance, in perfect agreement with the above data, silencing of TRPV3 counteracted the effects of eugenol and 2-APB to suppress growth (**Figure 4d**) and to stimulate apoptosis (**Figure 4e**) of ORS keratinocytes which data unambiguously verified the specific involvement of TRPV3 in mediating the cellular actions of these agents.

DISCUSSION

Uncovering the as yet ill-characterized functions of various TRP channels in human skin biology and pathology is an important, integral part of the ongoing exploration of the emerging roles of these molecules in regulatory mechanisms of non-neuronal tissues and cells (Clapham, 2003; Nilius et al., 2007; Szállási and Blumberg, 1999; Caterina and Julius, 2001; Paus et al., 2006a; Bíró et al., 2007). In this context, we provide the first evidence that TRPV3, by suppressing HF keratinocyte proliferation and inducing apoptosis-driven catagen regression, inhibits *in vitro* human hair growth. Given that these effects were generated with intact components of a normal human mini-organ and under assay conditions that preserve *in vivo*-like key functions of this organ during the test period, our findings are both physiologically and clinically relevant. Therefore, our current results, which are perfectly in line with previous data obtained on various mouse models (Asakawa et al., 2006; Xiao et al., 2008; Cheng et al., 2010; Steinhoff and Bíró, 2009; Imura et al., 2007), introduces TRPV3 as a significant novel player in human hair growth and cycling control.

That TRPV3 is functionally expressed in well-defined epithelial cellular compartments of the human HF is supported by numerous lines of evidence obtained on primary cultures of ORS keratinocytes. Indeed, plant-derived and synthetic TRPV3 activators induced membrane currents and elevations of $[Ca^{2+}]_{ic}$ which were effectively abrogated by the suppression of $[Ca^{2+}]_{ec}$ or by the co-administration of the nonselective TRP channel blocker ruthenium red. Of further importance, cellular effects of the TRPV3 activators (i.e. inhibition of proliferation, induction of apoptosis) were also inhibited by these manipulations and, of greatest importance, by the RNAi

mediated silencing of TRPV3 expression in these cells. Taken together, these data strongly argue for that a "TRPV3 channel opening → Ca^{2+} influx → growth arrest and apoptosis of ORS keratinocytes → hair growth inhibition" signaling pathway operates in the human HF.

Previously, the functional expression of TRPV3 was mostly identified on (mouse) epidermal keratinocytes. Indeed, TRPV3-specific heat and pharmacological agent-activated membrane currents and $[Ca^{2+}]_{ic}$ elevations were identified in these cells (Peier et al., 2002; Xiao et al., 2008; Cheng et al., 2010, Chung et al., 2004a, 2004b; Huang et al., 2008). In addition, stimulation of TRPV3 on keratinocytes induced the release of various mediators (e.g. interleukin 1α, prostaglandin E2, ATP) (Xu et al., 2006; Huang et al., 2008; Mandadi et al., 2009) which, as "intercellular messengers", were shown to activate pain and/or itch sensitive sensory afferents (Huang et al., 2008; Mandadi et al., 2009). However, these mediators are recognized proinflammatory agents in the skin (Bíró et al., 1998b, 2007; Paus and Cotsarelis, 1999; Stenn and Paus, 2001; Paus et al., 2006b); hence, TRPV3 channels expressed on keratinocytes were suggested to play a role in cutaneous inflammation. Indeed, transgenic overexpression of a "gain-of-function" mutant of the *trpv3* gene in epidermal keratinocytes of mice resulted in not only pruritus but severe dermatitis as well (Yoshioka et al., 2009). Furthermore, our preliminary data suggest that activation of TRPV3 significantly suppresses growth of human epidermal keratinocytes (Bíró et al., manuscript in preparation). These intriguing findings, along with our current presentation on the role of TRPV3 in human (and mouse) hair growth control, underscore the key physiological and pathophysiological significance of TRPV3, its

elusive endogenous ligands, and the coupled signaling mechanisms in multiple cellular compartments of the skin.

Of further importance, we and others have identified almost identical cutaneous regulatory mechanisms with the central involvement of another TRP channel, i.e. TRPV1. Indeed, stimulation of TRPV1 was shown to inhibit human (and murine) hair growth, promote premature catagen regression of the human HF, suppress proliferation and induce apoptosis of human epidermal and ORS keratinocytes, and induce the release of pro-inflammatory cytokines from these cells (Southall et al., 2003; Bodó et al., 2005; Bíró et al., 2006). It appears, therefore, that TRPV3-coupled signaling mechanisms (similar to those initiated by the activation of cutaneous TRPV1) act as key regulators of human hair growth and cycling and, most probably, other key biological processes of the skin.

In various heterologous systems ectopically expressing certain TRPs, the TRPV3 activator 2-APB was shown to be able to activate TRPV1 (Hu et al., 2004) (and possibly other TRP channels as well). However, according to our best knowledge, there is no data available on the effect of 2-APB on endogenous TRPV1 expressed by cultured human or mouse keratinocytes. Since (1) various agents may exert completely different affinities to “naïve” and “expressed” channels; and (2) we have previously shown that the activation of TRPV1 by capsaicin on human ORS keratinocytes induced TRPV1-specific influx of Ca^{2+} (Bodó et al., 2005), arguing for the functional expression of TRPV1 channels in the surface membrane of the ORS keratinocytes; our results that TRPV3 siRNA treatment completely abolished the effects of 2-APB suggest that the effects of 2-APB to increase $[Ca^{2+}]_{ic}$ and induce

membrane current in ORS keratinocytes is most probably mediated by TRPV3 and not by TRPV1.

Collectively, our findings may also have therapeutic implications. Our current presentation that stimulation of TRPV3 in the HF inhibits human hair growth suggests that (e.g. topically applied) TRPV3 agonists might become exploitable as novel, well-tolerated agents for the clinical management of unwanted hair growth (hirsutism). Likewise, future studies are now warranted to explore whether TRPV3 antagonists can be effectively employed in the treatment of various forms of hair loss (effluvium, alopecia). Finally, our data also invites one to systemically explore in future studies how the pro-inflammatory, pruritogenic, and anti-proliferative TRPV3 signaling in the skin can be manipulated in a clinically desired manner by endogenous and exogenous ligands in the management of relevant dermatoses such as e.g., psoriasis, certain forms of dermatitis, or even skin tumors. Therefore, clinicians who apply agents that activate and/or sensitize TRPV3 (e.g. camphor) (Xu et al., 2002; Peier et al., 2002) now need to take the above into account.

MATERIALS AND METHODS

Materials

Eugenol, carvacrol, thymol, and 2-aminoethoxydiphenyl borate (2-APB) were purchased from Sigma-Aldrich (St. Louis, MO).

Isolation and maintenance of HFs

The study was approved by the Institutional Research Ethics Committees and adhered to Declaration of Helsinki guidelines. Human anagen VI HFs (n=18–24 per group) were isolated from skin obtained from males undergoing hair transplantation or females undergoing face-lift surgery as we have described before (Bodó et al., 2005, 2009; Telek et al., 2007; Ramot et al., 2010). Isolated HFs were maintained in Williams' E medium (Invitrogen, Paisley, UK) supplemented with 2 mM L-glutamine (Invitrogen), 10 ng/ml hydrocortisone, 10 µg/ml insulin, and antibiotics (all from Sigma-Aldrich). Medium was changed every other day whereas treatment with various TRPV3 activators was performed daily. Length measurements were performed on individual HFs using a light microscope with an eyepiece measuring graticule.

Histology

Cryostat sections (6 µm) of cultured HFs were fixed in acetone, air-dried, and processed for histology. Hematoxylin and eosin (HE, Sigma-Aldrich) staining was

used for studying HF morphology and hair cycle stage (anagen, catagen) of each HF was assessed according to defined morphological criteria (Bodó et al., 2005, 2009; Telek et al., 2007; Ramot et al., 2010).

ORS keratinocyte cultures

Anagen HFs were digested using trypsin to obtain ORS keratinocytes (Bodó et al., 2005; Ramot et al., 2010; Limat and Noser, 1986). Similarly, human dermal fibroblasts (HDFs) were obtained from de-epidermized dermis using enzymatic digestion. ORS cultures were kept on feeder layer of mitomycin-treated HDFs (Bodó et al., 2005; Limat et al., 1989) in a 1:3 mixture of Ham's F12 and Dulbecco's modified Eagle's medium (both from Invitrogen) supplemented with 0.1 nM cholera toxin, 5 µg/ml insulin, 0.4 µg/ml hydrocortisone, 2.43 µg/ml adenine, 2 nM triiodothyronine, 10 ng/ml epidermal growth factor, 1 mM ascorbyl-2-phosphate, and antibiotics (all from Sigma-Aldrich).

Immunolabeling of TRPV3

For the detection of TRPV3 on isolated HFs and ORS keratinocytes, we performed fluorescent immunolabeling (Bodó et al., 2005, 2009; Telek et al., 2007; Ramot et al., 2010; Poeggeler et al., 2010). Cryostat HF sections or acetone-fixed ORS keratinocytes growing on coverslips were first incubated with primary antibody (1:200, overnight) against TRPV3 (Abcam, Cambridge, UK) and then with Alexa Fluor 488 dye-conjugated secondary antibody (Invitrogen) according to standard procedures. In addition, cultured ORS keratinocytes were identified by cytokeratin 7

(CK7) immunolabeling using a mouse monoclonal anti-CK7 antibody (1:100, Novus Biologicals, Cambridge, UK) and Alexa Fluor 568 dye-conjugated secondary antibody (Invitrogen). Nuclei were counterstained with Vectashield mounting medium containing DAPI (Vector Laboratories, Burlingame, CA). Images were acquired with an Eclipse E600 fluorescent microscope (Nikon, Tokyo, Japan). As negative controls, the appropriate primary antibodies were either omitted from the procedure or were preabsorbed with synthetic blocking peptides. In addition, the specificity of TRPV3 staining was also measured on tissues recognized to be positive for the channel; i.e. human epidermal skin sections (Gopinath et al., 2005; Facer et al., 2007) as well as normal human epidermal and HaCaT keratinocyte cultures (Sherkheli et al., 2009) (data not shown).

Ki-67/TUNEL double labeling

To evaluate apoptotic cells in the HFs in co-localization with a proliferation marker Ki-67, a Ki-67/TUNEL (terminal deoxynucleotidyl transferase biotin-dUTP nick end labeling) double-staining method was employed (Bodó et al., 2005, 2009; Telek et al., 2007). Cryostat sections were fixed in formalin/ethanol/acetic acid and labeled with a digoxigenin-deoxyUTP (ApopTag Fluorescein In Situ Apoptosis detection kit; Millipore, Billerica, MA) in presence of terminal deoxynucleotidyl transferase (TdT), followed by incubation with a mouse anti-Ki-67 antiserum (DAKO, Carpinteria, CA). TUNEL+ cells were visualized by an anti-digoxigenin FITC-conjugated antibody (ApopTag kit), whereas Ki-67 was detected by an Alexa Fluor 568 dye-conjugated secondary antibody (Invitrogen). Negative controls were performed by omitting TdT and the Ki-67 antibody. The number of cells positive for Ki-67 and TUNEL

immunoreactivity was counted per hair bulb and was normalized to the number of total (DAPI+) cells.

Quantitative "real-time" PCR (Q-PCR)

Q-PCR was performed on an ABI Prism 7000 sequence detection system (Applied Biosystems, Foster City, CA) by using the 5' nuclease assay as we have previously described (Bodó et al., 2005, 2009; Telek et al., 2007; Ramot et al., 2010; Poeggeler et al., 2010). Total RNA was isolated using TRIzol reagent (Invitrogen) according to manufacturer's protocol. Three µg of total RNA were then reverse-transcribed into cDNA by using 15 U of AMV reverse transcriptase (Promega, Madison, WI) and 0.025 µg/µl random primers (Promega). PCR amplification was performed by using the TaqMan primers and probes (TRPV3, assay ID, Hs00376854_m1) using the TaqMan universal PCR master mix protocol (Applied Biosystem). As internal controls, transcripts of glyceraldehyde 3-phosphate dehydrogenase (GAPDH, assay ID Hs99999905_m1) and cyclophylin (PPIA, assay ID Hs99999904_m1) were determined.

Western blotting

To determine the expression of TRPV3 in different keratinocyte cell types, the Western blot technique was applied (Bíró et al., 1998a, 1998b; Bodó et al., 2004, 2005; Telek et al., 2007). Cell lysates of ORS and HaCaT keratinocytes (the latter cells were used as positive controls) (Sherkheli et al., 2009) were subjected to SDS-PAGE, transferred to BioBond nitrocellulose membranes (Whatman, Maidstone, UK),

and then probed with the above anti-TRPV3 antibody (1:500, AbCam). A horseradish peroxidase polymer-conjugated anti-rabbit IgG antibody (Envision labeling, DAKO) were used as a secondary antibody, and the immunoreactive bands were visualized by SuperSignal West Pico Chemiluminescent Substrate-enhanced chemiluminescence (Pierce, Rockford, IL) using a Gel Logic 1500 Imaging System (Kodak, Tokyo, Japan). Negative control was performed by omitting the primary antibody.

Microfluorimetric measurements of $[Ca^{2+}]_i$

ORS keratinocyte cells were seeded in 96-well black-well/clear-bottom plates (Greiner Bio-One, Kremsmuenster, Austria) at a density of 20000 cells/well on mitomycin treated HDF feeder cells (900 cells/well) in ORS keratinocyte medium, supplemented as above, and cultured at 37°C for 24 hrs. The cells were then loaded with the cytoplasmic calcium indicator 2 μM Fluo-4 AM (Invitrogen) at 37°C for 30 min in Hank's Balanced Salt Solution (HBSS, Invitrogen) supplemented with 1% bovine serum albumin and 2.5 mM probenecid (both from Sigma-Aldrich). The cells were washed and finally kept in supplemented HBSS for 30 min at 37°C. The plates were then placed into a FlexStation II^{384} Fluorescence Imaging Plate Reader (FLIPR, Molecular Devices, Sunnyvale, CA) and changes in $[Ca^{2+}]_i$ (reflected by changes in fluorescence; λ_{EX}=494 nm, λ_{EM}=516 nm) induced by various concentrations of the drugs were recorded in each well (during the measurement, cells in a given well were exposed to only one given concentration of the agent). Experiments were performed in quadruplets and the averaged data (±SEM) were used in the calculations (Marincsák et al., 2008; Tóth et al., 2009a).

Patch-clamp experiments

ORS keratinocytes growing on 1 cm diameter coverslips were placed in a temperature controlled perfusion chamber mounted on a stage of an inverted Nikon microscope. All experiments were conducted at 37°C. Currents were recorded from cells superfused with Tyrode's solution containing (in mM) NaCl 140, KCl 5.4, $CaCl_2$ 2.5, $MgCl_2$ 1.2, HEPES 5, glucose 10, at pH 7.4. 2-APB was added to this superfusate from a 1 M stock solution in DMSO reaching a final concentration of 100 µM. Suction pipettes, fabricated from borosilicate glass, had tip resistances of 2-4 MW after filling with pipette solution composed of (in mM) K-aspartate 100, KCl 45, MgCl2 1, HEPES 5, EGTA 10, K-ATP 3. The pH of this solution was adjusted to 7.2 with KOH. Membrane currents were recorded with a Multiclamp-700A intracellular amplifier (Axon Instruments, Molecular Devices) using the whole cell configuration of the patch clamp technique (Hamill et al., 1981). After establishing high (>1 GΩ) resistance seal by gentle suction, the cell membrane beneath the tip of the electrode was disrupted by further suction and/or by applying 1.5 V electrical pulses for 1 ms. Ion currents were normalized to cell capacitance, determined in each cell using short hyperpolarizing pulses from –10 mV to –20 mV. Average cell capacitance was 34.5±2.5 pF whereas the series resistance was typically 5-10 MΩ and left uncompensated. Experiments were discarded when the amplitude of the measured current was unstable within the initial 5 min of the experiment, or the series resistance was high or increased during the measurement. Outputs from the clamp amplifier were digitized at 10 kHz using an A/D converter (Digidata-1322A, Axon

Instruments) under software control (pClamp 9.0, Axon Instruments) (Gönczi et al., 2007).

Determination of cellular proliferation

The degree of cellular growth (reflecting number of viable cells) was determined by measuring the DNA content of cells using CyQUANT Cell Proliferation Assay Kit (Invitrogen). ORS keratinocytes (10000 cells/well) were cultured on mitomycin treated HDF feeder cells (900 cells/well) in 96-well black-well/clear-bottom plates (Greiner Bio One) in quadruplicates and were treated with various compounds for the time indicated. Supernatants were then removed by blotting on paper towels, and the plates were subsequently frozen at –70°C. The plates were then thawed at room temperature, and 200 µl of CyQUANT dye/cell lysis buffer mixture was added to each well. After 5 min incubation, fluorescence was measured at 490 nm excitation and 520 nm emission wavelengths using FLIPR (Molecular Devices) (Tóth et al., 2009b).

Determination of apoptosis

A decrease in the mitochondrial membrane potential is one of the earliest markers of apoptosis (Green and Reed, 1998; Susin et al., 1998). Mitochondrial membrane potential of ORS keratinocytes was determined using a MitoProbe $DiIC_1(5)$ Assay Kit (Invitrogen) using our previously optimized protocols (Tóth et al., 2009b; Dobrosi et al., 2008). Cells were cultured and treated as described above. After removal of supernatants, cells were incubated for 30 minutes with $DiIC_1(5)$ working solution and

the fluorescence of $DiIC_1(5)$ was measured at 630 nm excitation and 670 nm emission wavelengths using the above FLIPR.

Determination of necrosis

Necrotic cell death was determined by SYTOX Green nucleic acid staining (Invitrogen). The dye is able to penetrate only to necrotic cells with ruptured plasma membranes, whereas healthy cells with intact surface membranes show negligible staining. Cells were cultured and treated as described above. Supernatants were then discarded and the cells were incubated with 1 µM SYTOX Green solution. Fluorescence of SYTOX Green was measured at 490 nm excitation and 520 nm emission wavelengths using a FLIPR (Tóth et al., 2009b; Dobrosi et al., 2008).

RNA interference (RNAi)

ORS keratinocytes were transfected by the Neon Transfection System (Invitrogen) using the Neon Kit according to manufacturer's instructions. Briefly, cells were harvested by trypsinization, washed and suspended in Resuspension buffer (Invitrogen). Two TRPV3-specific Stealth RNAi oligonucleotides (IDs: HSS136316 and HSS175965, 40 nM, Invitrogen) as well as RNAi Negative Control Duplexes (Scrambled RNAi, Invitrogen) were transfected to the cells by electroporation (settings: 900 V, 20 ms, two times). Transfected cells were then plated into 35 mm Petri dishes for verification and 96 well plates for other assays. The efficacy of siRNA-driven knockdown (**Supplementary Figure 1.**) was daily evaluated by Western blot analysis and Ca-imaging for 4 days as we have described before (Tóth

et al., 2009b; Dobrosi et al., 2008; Griger et al., 2007). In all cases, the specific RNAi probes resulted in >70% suppression of the expression of TRPV3 by day 2 and remained suppressed for 2 additional days (data not shown). Hence, experiments were performed 2 days after transfection.

Statistical analysis

When applicable, data were analyzed using a two-tailed unpaired *t*-test (except for analyzing the patch-clamp data where Student's *t*-test for paired data was applied) and $p<0.05$ values were regarded as significant differences.

CONFLICT OF INTEREST

The authors state no conflict of interest.

ACKNOWLEDGEMENTS

This work was supported in part by Hungarian (OTKA NK78398, OTKA NNF78456) and EU (FP7-REGPOT-2008-1/22992) research grants for TB and by the Deutsche Forschungsgemeinschaft to RP. In addition, the work is supported by the TÁMOP 4.2.2-08/1/2008-0019 and TÁMOP 4.2.1./B-09/1/KONV-2010-0007 projects and is implemented through the „New Hungary Development Plan", co-financed by the European Social Fund. TB and CG are recipients of the János Bolyai scholarship of the Hungarian Academy of Sciences.

REFERENCES

Amann R, Maggi CA (1991) Ruthenium red as a capsaicin antagonist. *Life Sci* 49:849-856.

Asakawa M, Yoshioka T, Matsutani T, *et al* (2006) Association of a mutation in TRPV3 with defective hair growth in rodents. *J Invest Dermatol* 126:2664-2672.

Bíró T, Bodó E, Telek A, *et al* (2006) Hair cycle control by vanilloid receptor-1 (TRPV1): evidence from TRPV1 knockout mice. *J Invest Dermatol* 126:1909-1912.

Bíró T, Brodie C, Modarres S, *et al* (1998a) Specific vanilloid responses in C6 rat glioma cells. *Brain Res Mol Brain Res* 56:89-98.

Bíró T, Maurer M, Modarres S, *et al* (1998b) Characterization of functional vanilloid receptors expressed by mast cells. *Blood* 91:1332-1340.

Bíró T, Tóth BI, Marincsák R, *et al* (2007) TRP channels as novel players in the pathogenesis and therapy of itch. *Biochim Biophys Acta* 1772:1004-1021.

Bodó E, Bíró T, Telek A, *et al* (2005) A hot new twist to hair biology: involvement of vanilloid receptor-1 (VR1/TRPV1) signaling in human hair growth control. *Am J Pathol* 166:985-998.

Bodó E, Kovács I, Telek A, *et al* (2004) Vanilloid receptor-1 (VR1) is widely expressed on various epithelial and mesenchymal cell types of human skin. *J Invest Dermatol* 123:410-413.

Bodó E, Kromminga A, Bíró T, *et al* (2009) Human female hair follicles are a direct, nonclassical target for thyroid-stimulating hormone. *J Invest Dermatol* 129:1126-1139.

Caterina MJ, Julius D (2001) The vanilloid receptor: a molecular gateway to the pain pathway. *Annu Rev Neurosci* 24:487-517.

Cheng X, Jin J, Hu L, *et al* (2010) TRP channel regulates EGFR signaling in hair morphogenesis and skin barrier formation. *Cell* 141:331-343.

Chung MK, Lee H, Mizuno A, *et al* (2004a) 2-aminoethoxydiphenyl borate activates and sensitizes the heat-gated ion channel TRPV3. *J Neurosci* 24:5177-5182.

Chung MK, Lee H, Mizuno A, *et al* (2004b) TRPV3 and TRPV4 mediate warmth-evoked currents in primary mouse keratinocytes. *J Biol Chem* 279:21569-21575.

Clapham DE (2003) TRP channels as cellular sensors. *Nature* 426:517-524.

Denda M, Fuziwara S, Inoue K, *et al* (2001) Immunoreactivity of VR1 on epidermal keratinocyte of human skin. *Biochem Biophys Res Commun* 285:1250-1252.

Dobrosi N, Tóth BI, Nagy G, *et al* (2008) Endocannabinoids enhance lipid synthesis and apoptosis of human sebocytes via cannabinoid receptor-2-mediated signaling. *FASEB J* 22:3685-3695.

Facer P, Casula MA, Smith GD, *et al* (2007) Differential expression of the capsaicin receptor TRPV1 and related novel receptors TRPV3, TRPV4 and TRPM8 in normal human tissues and changes in traumatic and diabetic neuropathy. *BMC Neurol* 7:11.

Gönczi M, Szentandrássy N, Fülöp L, *et al* (2007) Hypotonic stress influence the membrane potential and alter the proliferation of keratinocytes in vitro. *Exp Dermatol* 16:302-310.

Gopinath P, Wan E, Holdcroft A, *et al* (2005) Increased capsaicin receptor TRPV1 in skin nerve fibres and related vanilloid receptors TRPV3 and TRPV4 in keratinocytes in human breast pain. *BMC Womens Health* 5:2.

Green DR, Reed JC (1998) Mitochondria and apoptosis. *Science* 281:1309-1312.

Griger Z, Páyer E, Kovács I, *et al* (2007) Protein kinase C-beta and -delta isoenzymes promote arachidonic acid production and proliferation of MonoMac-6 cells. *J Mol Med* 85:1031-1042.

Hamill OP, Marty A, Neher E, *et al* (1981) Improved patch-clamp techniques for high-resolution current recording from cells and cell-free membrane patches. *Pflugers Arch* 391:85-100.

Hu HZ, Gu Q, Wang C, Colton CK *et al* (2004) 2-aminoethoxydiphenyl borate is a common activator of TRPV1, TRPV2, and TRPV3. *J Biol Chem.* 279:35741-8.

Huang SM, Lee H, Chung MK, *et al* (2008) Overexpressed transient receptor potential vanilloid 3 ion channels in skin keratinocytes modulate pain sensitivity via prostaglandin E2. *J Neurosci* 28:13727-13737.

Imura K, Yoshioka T, Hikita I, *et al* (2007) Influence of TRPV3 mutation on hair growth cycle in mice. *Biochem Biophys Res Commun* 363:479-483.

Limat A, Hunziker T, Boillat C, *et al* (1989) Post-mitotic human dermal fibroblasts efficiently support the growth of human follicular keratinocytes. *J Invest Dermatol* 92:758-762.

Limat A, Noser FK (1986) Serial cultivation of single keratinocytes from the outer root sheath of human scalp hair follicles. *J Invest Dermatol* 87:485-488.

Lindner G, Botchkarev VA, Botchkareva NV, *et al* (1997) Analysis of apoptosis during hair follicle regression (catagen). *Am J Pathol* 151:1601-1617.

Mandadi S, Sokabe T, Shibasaki K, *et al* (2009) TRPV3 in keratinocytes transmits temperature information to sensory neurons via ATP. *Pflugers Arch* 458:1093-1102.

Marincsák R, Tóth BI, Czifra G, *et al* (2008) The analgesic drug, tramadol, acts as an agonist of the transient receptor potential vanilloid-1. *Anesth Analg* 106:1890-1896.

Moussaieff A, Rimmerman N, Bregman T, *et al* (2008) Incensole acetate, an incense component, elicits psychoactivity by activating TRPV3 channels in the brain. *FASEB J* 22:3024-3034.

Müller-Röver S, Handjiski B, van der Veen C, *et al* (2001) A comprehensive guide for the accurate classification of murine hair follicles in distinct hair cycle stages. *J Invest Dermatol* 117:3-15.

Nilius B, Owsianik G, Voets T, *et al* (2007) Transient receptor potential cation channels in disease. *Physiol Rev* 87:165-217.

Paus R, Cotsarelis G (1999) The biology of hair follicles. *N Engl J Med* 341:491-497.

Paus R, Schmelz M, Bíró T, *et al* (2006a) Frontiers in pruritus research: scratching the brain for more effective itch therapy. *J Clin Invest* 116:1174-1186.

Paus R, Theoharides TC, Arck PC (2006b) Neuroimmunoendocrine circuitry of the 'brain-skin connection'. *Trends Immunol* 27:32-39.

Peier AM, Reeve AJ, Andersson DA, *et al* (2002) A heat-sensitive TRP channel expressed in keratinocytes. *Science* 296:2046-2049.

Poeggeler B, Knuever J, Gáspár E, *et al* (2010) Thyrotropin powers human mitochondria. *FASEB J* 24:1525-1531.

Ramot Y, Bíró T, Tiede S, *et al* (2010) Prolactin--a novel neuroendocrine regulator of human keratin expression in situ. *FASEB J* 24:1768-1779.

Sherkheli MA, Benecke H, Doerner JF, *et al* (2009) Monoterpenoids induce agonist-specific desensitization of transient receptor potential vanilloid-3 (TRPV3) ion channels. *J Pharm Pharm Sci* 12:116-128.

Slominski A, Wortsman J (2000) Neuroendocrinology of the skin. *Endocrine Rev* 21:457-487.

Smith GD, Gunthorpe MJ, Kelsell RE, *et al* (2002) TRPV3 is a temperature-sensitive vanilloid receptor-like protein. *Nature* 418:186-190.

Southall MD, Li T, Gharibova LS, *et al* (2003) Activation of epidermal vanilloid receptor-1 induces release of proinflammatory mediators in human keratinocytes. *J Pharmacol Exp Ther* 304:217-222.

Steinhoff M, Bíró T (2009) A TR(I)P to pruritus research: role of TRPV3 in inflammation and itch. *J Invest Dermatol* 129:531-535.

Stenn KS, Paus R (2001) Controls of hair follicle cycling. *Physiol Rev* 81:449-494.

Susin SA, Zamzami N, Kroemer G (1998) Mitochondria as regulators of apoptosis: doubt no more. *Biochim Biophys Acta* 1366:151-165.

Szállási A, Blumberg PM (1999) Vanilloid (Capsaicin) receptors and mechanisms. *Pharmacol Rev* 51:159-212.

Telek A, Bíró T, Bodó E, *et al* (2007) Inhibition of human hair follicle growth by endo- and exocannabinoids. *FASEB J* 21:3534-3541.

Tóth BI, Benkő S, Szöllősi AG, *et al* (2009a) Transient receptor potential vanilloid-1 signaling inhibits differentiation and activation of human dendritic cells. *FEBS Lett* 583:1619-1624.

Tóth BI, Géczy T, Griger Z, *et al* (2009b) Transient receptor potential vanilloid-1 signaling as a regulator of human sebocyte biology. *J Invest Dermatol* 129:329-339.

Xiao R, Tian J, Tang J, *et al* (2008) The TRPV3 mutation associated with the hairless phenotype in rodents is constitutively active. *Cell Calcium* 43:334-343.

Xu H, Delling M, Jun JC, *et al* (2006) Oregano, thyme and clove-derived flavors and skin sensitizers activate specific TRP channels. *Nat Neurosci* 9:628-635.

Xu H, Ramsey IS, Kotecha SA, *et al* (2002) TRPV3 is a calcium-permeable temperature-sensitive cation channel. *Nature* 418:181-186.

Yoshioka T, Imura K, Asakawa M, *et al* (2009) Impact of the Gly573Ser substitution in TRPV3 on the development of allergic and pruritic dermatitis in mice. *J Invest Dermatol* 129:714-722.

FIGURE LEGENDS

Figure 1. *TRPV3 is expressed in the epithelium of human HF and on cultured ORS keratinocytes*

Immunofluorescence (green) of TRPV3 in organ-cultured human HFs *in situ* (**a**) and on primary cultures of ORS keratinocytes (**b**). ORS, outer root sheath; DP, dermal papilla; MK, matrix keratinocytes. Scale bars, 50 µm (**a**) and 10 µm (**b**) ORS keratinocytes were identified by cytokeratin 7 (CK7) immunolabeling (red fluorescence). Nuclei were counterstained by DAPI (blue fluorescence). Insets: pre-absorption negative control (NC). (**c**) TRPV3 protein expression in human ORS and epidermal HaCaT keratinocytes, as determined by Western blotting. (**d**) TRPV3 mRNA expression in human anagen and catagen HFs, ORS keratinocytes (ORSK), DP fibroblasts (DPF), and dermal fibroblasts (HDF), as assessed by quantitative "real-time" PCR. Data are expressed as mean±SEM of 3 independent determinations performed in triplicate.

Figure 2. *In organ-cultured HFs, stimulation of TRPV3 inhibits human hair shaft elongation and intrafollicular proliferation, and induces apoptosis and premature catagen regression*

(**a**) Hair shaft elongation curves (18–24 HFs per group, mean±SEM). *p<0.05 when compared to control. (**b**) Co-immunolabeling of proliferating (Ki-67+, red fluorescence) and apoptotic (TUNEL+, green fluorescence) cells, along with nuclei (DAPI+, blue fluorescence). Statistical analysis of number of Ki-67+ and TUNEL+ cells as compared with the number of DAPI+ cells. (**c**) Quantitative hair cycle histomorphometry on hematoxylin-eosin-stained sections. Percentage of HF in anagen or catagen state was determined. (**b,c**) Data are expressed as mean±SEM.

*p<0.05 when compared to control. DP, dermal papilla, MK, matrix keratinocytes. Scale bars, 50 µm.

Figure 3. *TRPV3 is expressed as a Ca^{2+}-permeable ion channel on human ORS keratinocytes*

(**a**) Representative fluorimetric Ca^{2+}-imaging data recorded on Fluo-4 loaded ORS keratinocytes. The arrow indicates the application of 100 µM 2-APB and 300 µM eugenol in solutions containing normal (1.8 mM) or low (0.02 mM) [Ca^{2+}]. (**b**) Statistical analysis of maximal amplitudes of Ca^{2+}-elevations induced by the TRPV3 agonists in normal (1.8 mM) or low (0.02 mM) [Ca^{2+}] solutions, or in the presence of 10 µM ruthenium red (measured in normal [Ca^{2+}] solution). In all cases, mean±SEM of multiple determinations (n>3) are presented. For statistical analysis, * marks significant (p<0.05) differences compared to the control, whereas # marks significant (p<0.05) differences compared to the maximal TRPV3 activator-induced Ca^{2+}-elevations recorded in normal [Ca^{2+}] solution. (**c**) Representative IV curves recorded with a patch-clamp ramp protocol shown in the inset. (**d**) A usual time-course of a single experiment showing 100 µM 2-APB-induced current values measured at –40 mV (open symbols) and at +90 mV (filled symbols). (**e**) Statistical analysis of normalized currents to cell membrane capacitance (mean±SEM, n=7) measured at –40 mV (left side downward), +40 mV (left side upward), –90 mV (right side downward) and +90 mV (right side upward) in different conditions. (**f**) Statistical analysis of normalized currents in the presence and after washout of 100 µM 2-APB measured at –40 mV (left) and +90 mV (right) (mean±SEM, n=7). (**e,f**) * marks significant (p<0.05) differences compared to the control.

Figure 4. *Activations of TRPV3 on human ORS keratinocytes suppresses proliferation and induces cell death*

(**a**) ORS keratinocytes were treated with various concentrations of TRPV3 activators for 48 hrs medium containing normal (1.8 mM) [Ca^{2+}]. Proliferation was determined by a CyQUANT assay, apoptosis was assessed by a $DilC_1(5)$ assay reflecting (decreasing) mitochondrial membrane potential, and necrosis was determined by a Sytox Green assay. (**b,c**) The above treatment protocols were performed in low (0.02 mM) [Ca^{2+}] medium or in the presence of 10 μM ruthenium red (in normal [Ca^{2+}] medium), and alterations in proliferation (**b**) and apoptosis (**c**) were assessed. (**a-c**) Data (mean±SEM) are expressed as a percentage of the mean value (defined as 100 %) of the vehicle-treated control group. * marks significant ($p<0.05$) differences compared to the (1.8. mM [Ca^{2+}]) vehicle-treated control. (**b,c**) # marks significant ($p<0.05$) differences compared to the TRPV3 activator-treated group (measured in normal [Ca^{2+}] medium). (**d,e**) Two RNAi probes against TRPV3, as well as scrambled RNAi probes, were introduced to ORS keratinocytes. Two days after transfection, cells were treated by TRPV3 activators for 48 hrs, and alterations in proliferation (**d**) and apoptosis (**e**) were assessed. Data (mean±SEM) are expressed as a percentage of the mean value (defined as 100%) of the vehicle-treated non-transfected control group. For statistical analysis, * marks significant ($p<0.05$) differences compared to the Scrambled RNAi-treated group, whereas # marks significant ($p<0.05$) differences compared to the TRPV3 activator-stimulated Scrambled RNAi-treated group. In all cases, three-four additional experiments yielded similar results.

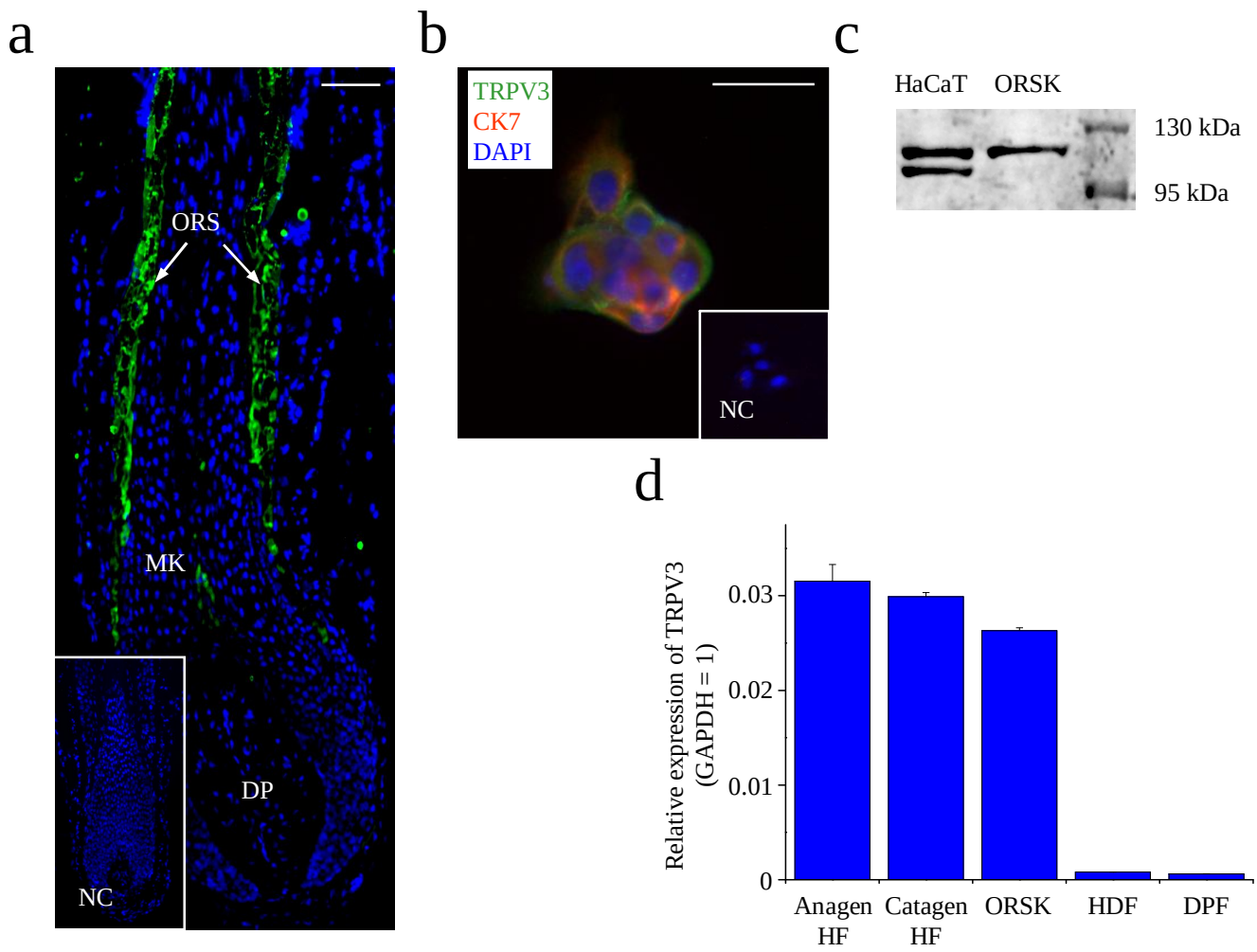
a
ORS
MK
DP
NC
b
TRPV3
CK7
DAPI
NC
c
HaCaT
ORSK
130 kDa
95 kDa
d
Relative expression of TRPV3
(GAPDH = 1)
0.03
0.02
0.01
0
Anagen HF
Catagen HF
ORSK
HDF
DPF

Figure 1

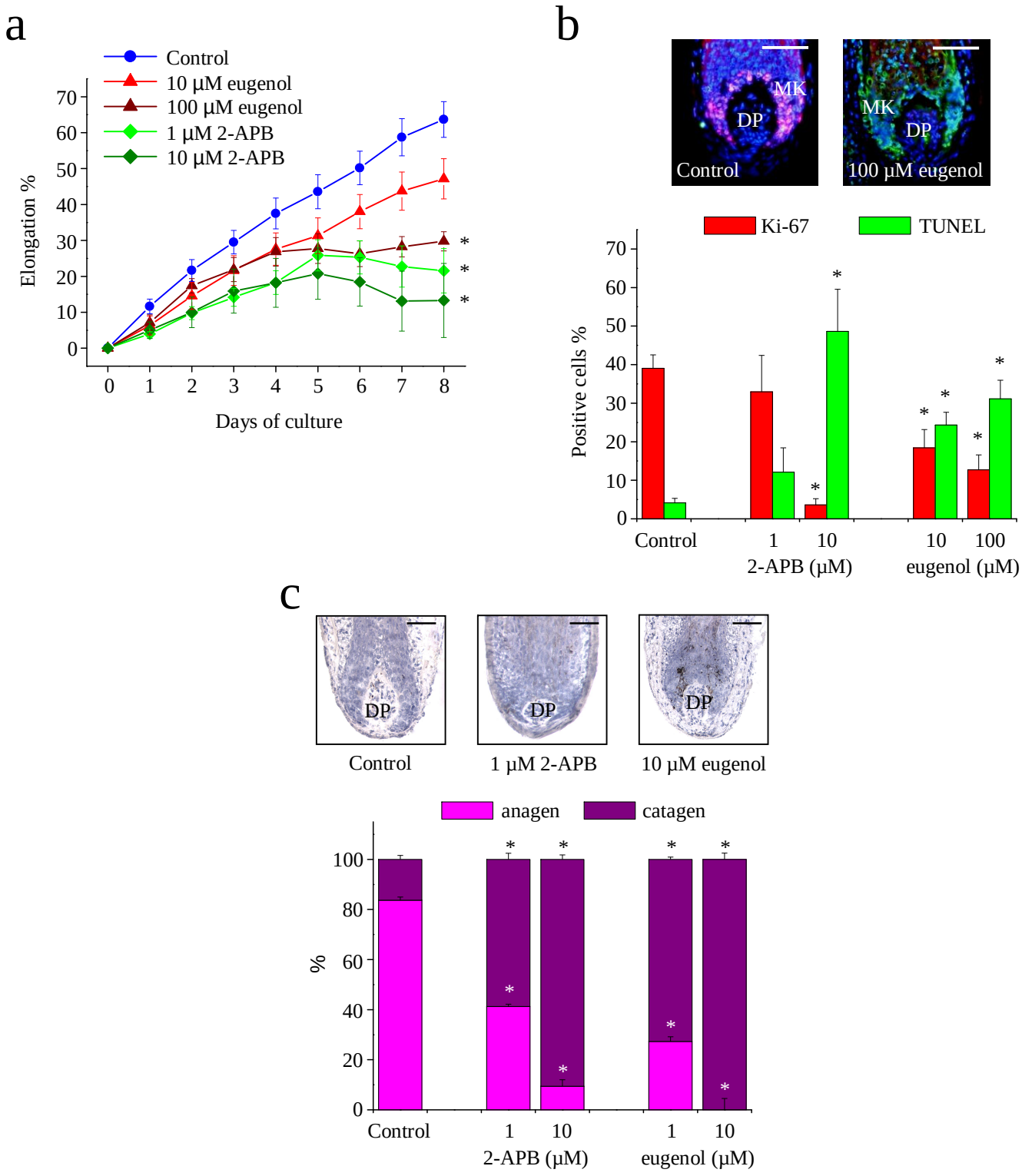
a
Control
10 µM eugenol
100 µM eugenol
1 µM 2-APB
10 µM 2-APB
Elongation %
Days of culture
b
MK
DP
Control
100 µM eugenol
Ki-67
TUNEL
Positive cells %
Control
2-APB (µM)
eugenol (µM)
c
DP
Control
1 µM 2-APB
10 µM eugenol
anagen
catagen
%
Control
2-APB (µM)
eugenol (µM)

Figure 2

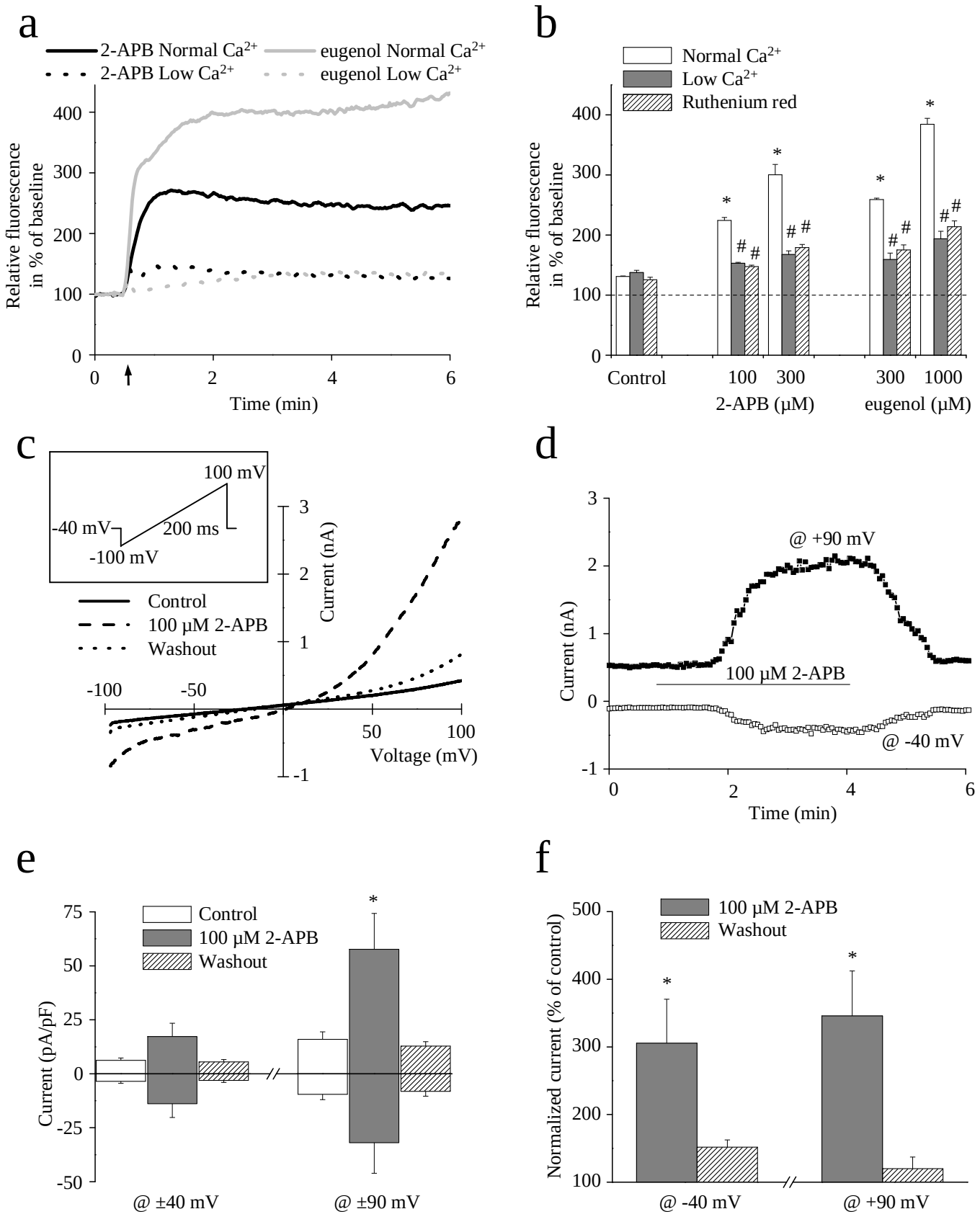
a
2-APB Normal Ca2+
2-APB Low Ca2+
eugenol Normal Ca2+
eugenol Low Ca2+
Relative fluorescence in % of baseline
Time (min)
b
Normal Ca2+
Low Ca2+
Ruthenium red
Relative fluorescence in % of baseline
Control
2-APB (µM)
eugenol (µM)
c
100 mV
-40 mV
200 ms
-100 mV
Control
100 µM 2-APB
Washout
Current (nA)
Voltage (mV)
d
@ +90 mV
100 µM 2-APB
@ -40 mV
Current (nA)
Time (min)
e
Control
100 µM 2-APB
Washout
Current (pA/pF)
@ ±40 mV
@ ±90 mV
f
100 µM 2-APB
Washout
Normalized current (% of control)
@ -40 mV
@ +90 mV

Figure 3

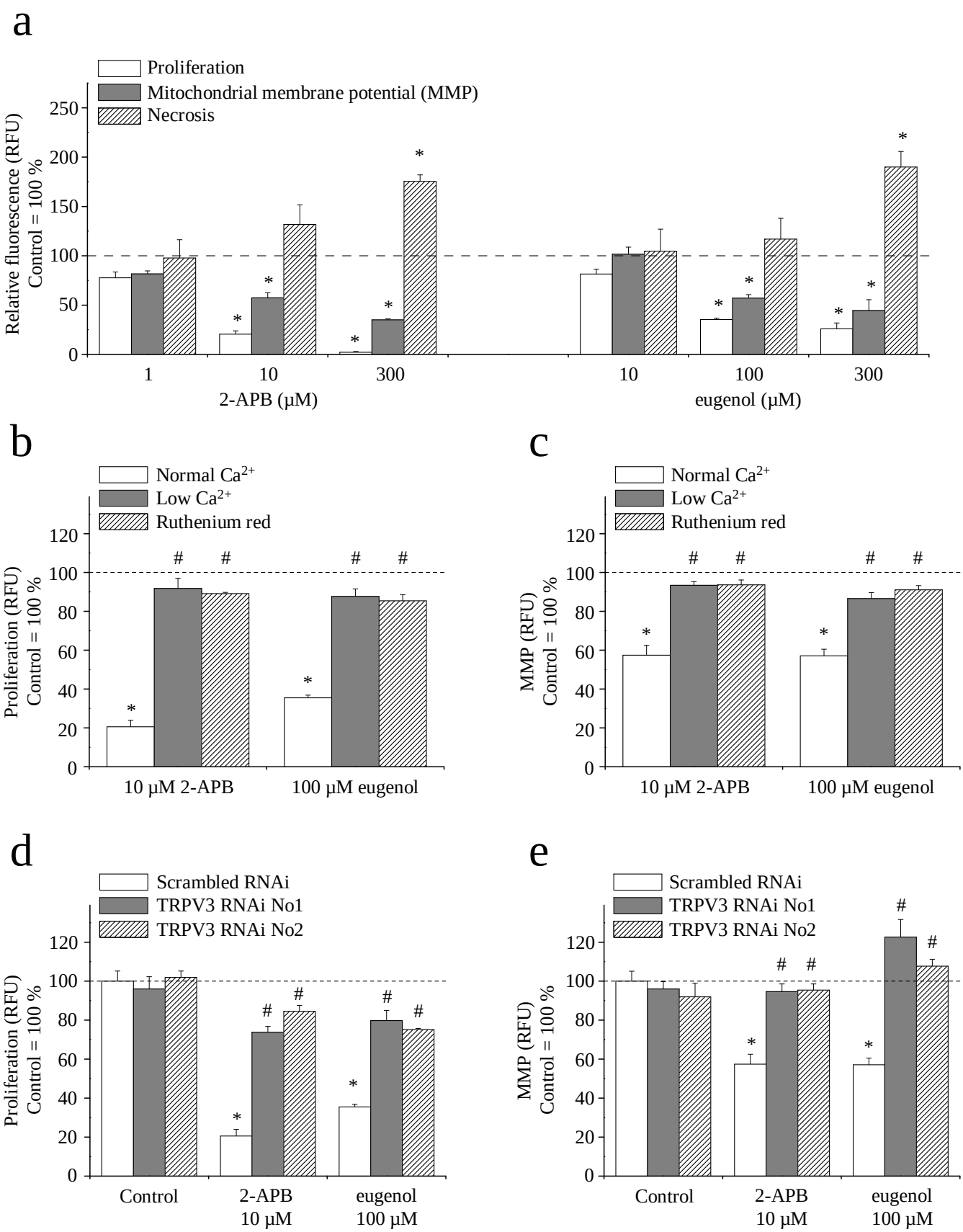
a
Proliferation
Mitochondrial membrane potential (MMP)
Necrosis
Relative fluorescence (RFU)
Control = 100 %
2-APB (μM)
eugenol (μM)
b
Normal Ca2+
Low Ca2+
Ruthenium red
Proliferation (RFU)
Control = 100 %
10 μM 2-APB
100 μM eugenol
c
MMP (RFU)
d
Scrambled RNAi
TRPV3 RNAi No1
TRPV3 RNAi No2
Control
2-APB 10 μM
eugenol 100 μM
e

Figure 4

SUPPLEMENTARY MATERIAL

SUPPLEMENTARY FIGURE LEGENDS

Supplementary Figure 1. *Evaluation of efficiency of RNAi-mediated knock-down of TRPV3 in cultured ORS keratinocytes*

Various RNAi probes against TRPV3 (indicated by numbers), as well as a scrambled RNAi probe, were introduced to ORS keratinocytes as described under “Materials and methods” (Control, transfection reagent-treated control group). To evaluate the efficacy of this intervention, at days 1-4 after transfection, cells were subjected to Western blot analysis (molecular evaluation) and Ca^{2+}-imaging (functional evaluation). (**a**) Representative Western blot results measured at day 2 after transfection. As a house-keeping molecule, to assess equal loading, expression of β-actin was also determined. Note that both TRPV3-specific RNAi probes employed markedly suppressed the expression of the protein. Two additional experiments yielded similar results. (**b**) Ca^{2+}-imaging data recorded at day 2 after transfection. Statistical analysis of maximal amplitudes of Ca^{2+}-elevations induced by the TRPV3 agonists in various Fluo-4-loaded ORS keratinocyte populations. In all cases, mean±SEM of multiple determinations are presented. For statistical analysis, * marks significant ($p<0.05$) differences compared to the maximal TRPV3 activator-induced Ca^{2+}-elevations measured on Control (transfection reagent-treated) cultures. Note that both 100 μM 2-APB and 300 μM eugenol induced significantly smaller Ca^{2+}-transients in TRPV3-RNAi transfected cells.

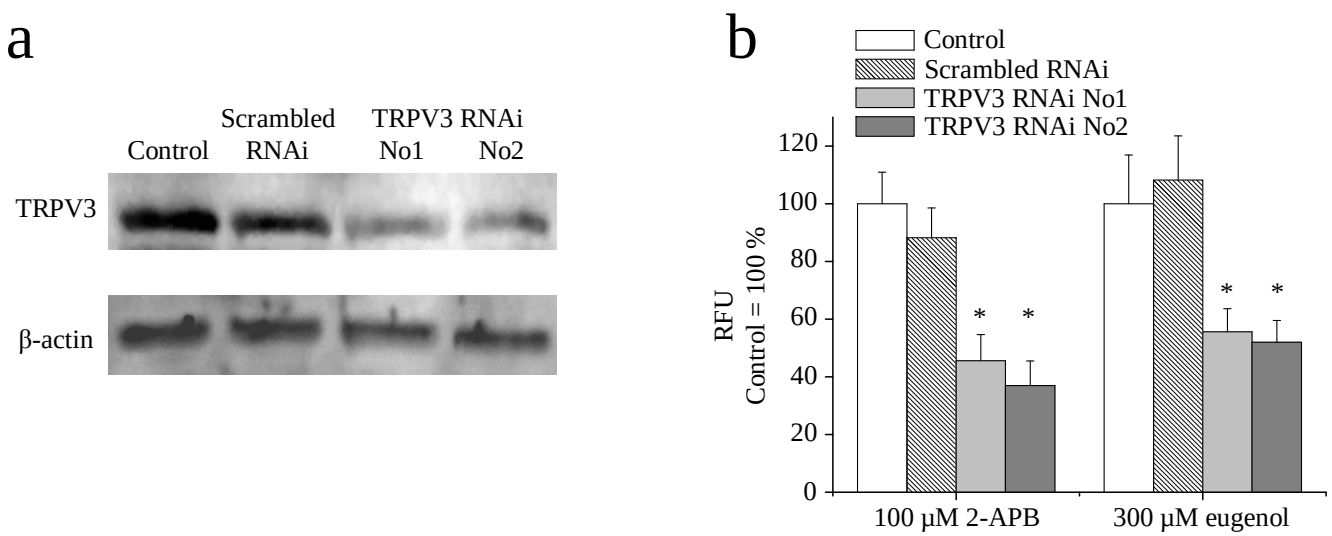

Supplementary Figure 1